CrossMark

Astrometric Reduction of Saturnian Satellites with Cassini-ISS Images Degraded by Trailed Stars

Qing-Feng Zhang[1,2], Meng-Qi Liu[1], Yan Li[1,2] , Lin-Peng Wu[1], Zhi-Qiang Wang[1], Li-Sha Zhu[3], and Zhan Li[1,2]
[1] Department of Computer Science, Jinan University, Guangzhou 510632, China; tyanei@jnu.edu.cn
[2] Sino-French Joint Laboratory for Astrometry, Dynamics and Space Science, Jinan University, Guangzhou 510632, China
[3] Department of Financial Technology, School of Management, Guangzhou Xinhua University, Guangzhou 510520, China

Abstract

The Imaging Science Subsystem (ISS) mounted on the Cassini spacecraft has taken a lot of images, which provides an important source of high-precision astrometry of some planets and satellites. However, some of these images are degraded by trailed stars. Previously, these degraded images cannot be used for astrometry. In this paper, a new method is proposed to detect and compute the centers of these trailed stars automatically. The method is then performed on the astrometry of ISS images with trailed stars. Finally, we provided 658 astrometric positions between 2004 and 2017 of several satellites that include Enceladus, Dione, Tethys, Mimas and Rhea. Compared with the JPL ephemeris SAT427, the mean residuals of these measurements are 0.11 km and 0.26 km in R.A. and decl., respectively. Their standard deviations are 1.08 km and 1.37 km, respectively. The results show that the proposed method performs astrometric measurements of Cassini ISS images with trailed stars effectively.

Key words: astrometry – planets and satellites: individual (Enceladus, Dione, Mimas, Rhea and Tethys) – techniques: image processing – methods: data analysis

1. Introduction

The Imaging Science Subsystem (ISS) is a piece of optic equipment mounted on the Cassini spacecraft (Porco et al. 2004). During the entire Cassini tour, it took more than 400,000 images. These images have provided a lot of astrometric data on the satellites of Saturn and Jupiter. For instance, Cooper et al. (2006) obtained the astrometric data of inner Jovian satellites from the early ISS images. Tajeddine et al. (2013, 2015) and Cooper et al. (2014) reduced a part of ISS images of several main Saturnian satellites. Zhang et al. (2018, 2021, 2022) measured some ISS images of several Saturnian satellites. These data have been used in the studies of the dynamics of planetary systems (Desmars et al. 2013; Cooper et al. 2015; Lainey et al. 2017, 2020). All these researches demonstrate the importance of the astrometry of ISS images.

In 2018, a standard and versatile tool for the astrometry of ISS images, Caviar, has been released to the community by Cooper et al. (2018). Caviar can reduce normal ISS images. However, it cannot cope with the degraded images with trailed stars because of the inability of detecting streaks and obtaining their centers. In astrometry, these streaks are expected to be used as reference stars to correct camera pointing. If they cannot be analyzed, the measurement of the image will fail. Otherwise, these degraded images will be valuable for astrometry and can provide more astrometric positions of celestial objects. Figure 1 shows four example images with

streaks. They are the ISS images of Mimas, Enceladus, Rhea and Dione, respectively. The streaks were caused by long exposure time or improper tracking.

In these days, detecting and centering streaks in astronomical images have been studied by various researchers. Laas-Bourez et al. (2009) proposed an algorithm based on mathematical morphology for detecting the trajectory of space debris and developed the software TAROT that can fully automated extracting source positions of objects in geostationary transfer orbit. It is dedicated to observations with two small TAROT telescopes. Sun et al. (2013) presented another mathematical morphology method to detect streaks of space debris and obtain its center. As a result, the astrometric precision of space debris is improved. However, the above two algorithms need predict the approximate direction or length of the object to define a structural element. It is not suitable for processing ISS images because the direction and length of streaks are unknown in ISS images. Virtanen et al. (2016) gave an automated streak detection and processing pipeline for the ESA-funded Streak-Det (streak detection and astrometric reduction) activity. Although its detection sensitivity for bright objects or objects longer than 100 pixels reaches 90%, the sensitivity for shorter ones is only 63%. Since the length of streaks in ISS images are mostly shorter than 100 pixels, the method is not suitable for ISS images. Sease et al. (2017) offered a method to automatically locate two endpoints of one streak according to corner metrics. However, the centering method of streak was
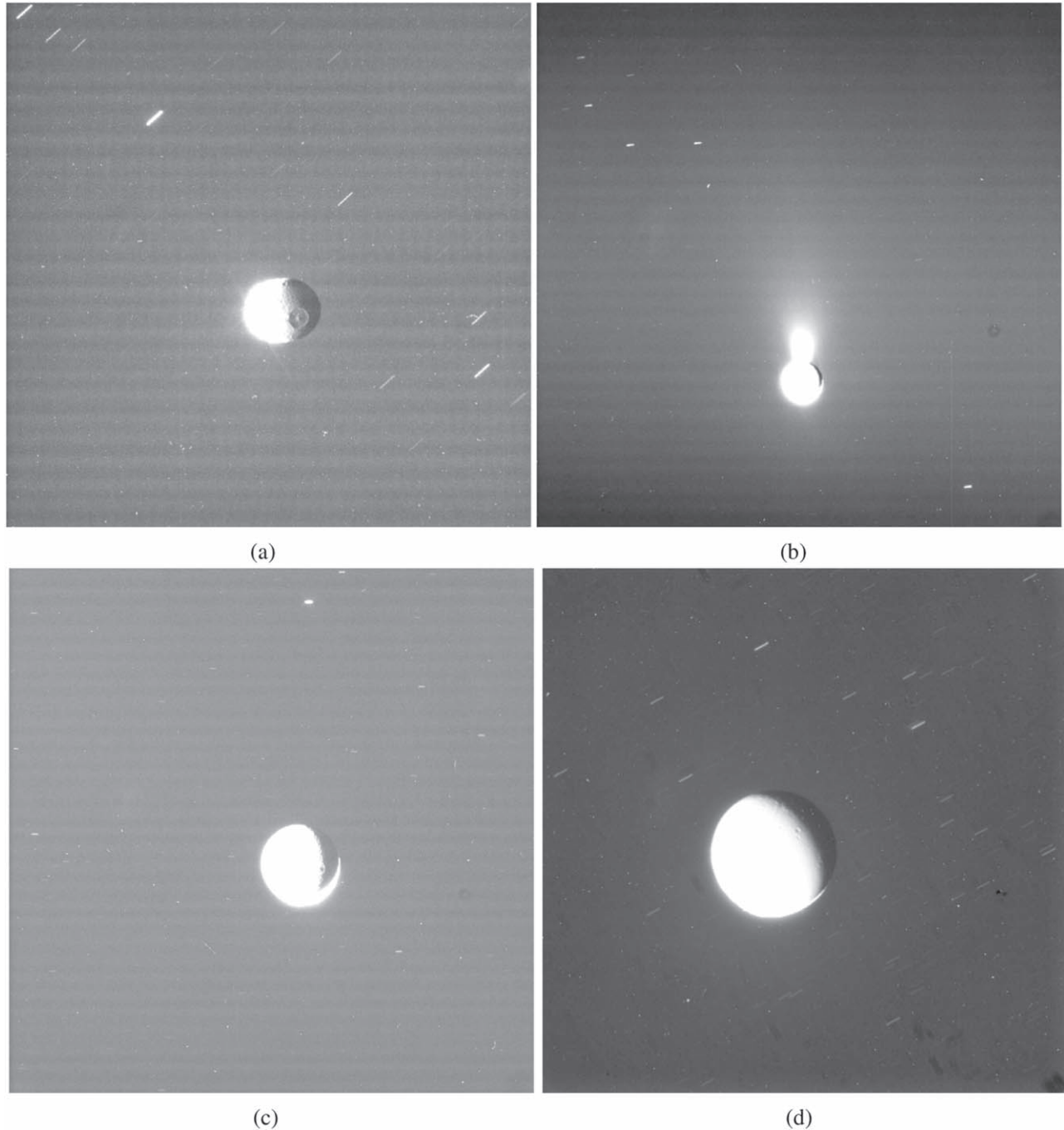
Figure 1. Some examples of ISS images in which all the stars are streaks. The images are enhanced by applying contrast stretching for visibility. (a) An image of Mimas (Image ID: N1743596513), (b) an image of Enceladus (Image ID: N1872048342), (c) an image of Rhea (Image ID: N1516373834), (d) an image of Dione (Image ID: N1880313867).

not provided, and the endpoints locating method was tested only on the simulated images. In addition, there are some famous processing systems that contain the function of detecting and centering streaks. For example, Pan-STARRS Moving Object Processing System (MOPS) (Denneau et al. 2013) and TRailed Image Photometry in Python (TRIPPy) (Fraser et al. 2016). All these methods and pipelines are not suitable for the astrometry of ISS images because most of them are dedicated to some specific equipment, or to a specific project, or aiming at photometry.
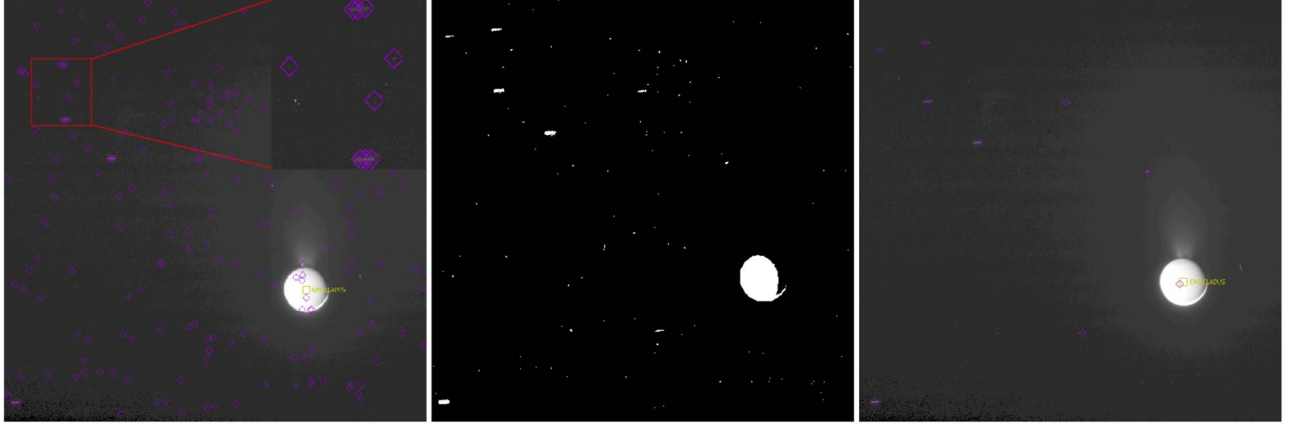
Figure 2. The results of the three steps with a trailed star degraded image. (Left) Searched peak points. (Middle) Detected streaks. (Right) Streaks and their centers.

In this paper, a method that can automatically detect and center all streaks in an ISS image is first proposed, the method is then applied to the astrometry of ISS images with trailed stars of several main Saturnian satellites. The remaining of this paper is organized as follows. An introduction to our streak centering method is presented in Section 2. Section 3 describes the astrometry of several moons of Saturn. Section 4 provides a discussion about our method and measurements. The conclusions are given in Section 5.

2. Streak Centering

In the astrometry of ISS images with trailed stars, the key problem is to determine the accurate centers of streaks. There are three main steps in our method to solve the problem, including searching peak points, finding streaks and centering streaks. Details are given below.

2.1. Step 1: Searching Peak Points

Stetson (1987) published a classical package of photometry, DAOPHOT, which includes a routine FIND. The FIND routine is very powerful in searching stars in an image. Its principle is to find stars as the points with local maxima in an image H that is generated by convolving an original image F with a truncated Gaussian function, and obtain the star centers by fitting a bivariate Gaussian function to the intensity distribution over their neighborhood in F. If the stars are point-like, the FIND routine can identify them and output their centers accurately. However, FIND cannot handle the trailed stars correctly. That is, a trailed star may not be found, or may be recognized as one or more stars. Even when the streak is recognized as one star, its center cannot be located correctly.

In this step, the aim is to locate at least one peak point in each streak in image H. The peak points will be the input of the next step. Since the streaks of stars in the ISS images are longer than normal point sources, to detect peak points successively

the FIND parameter settings should be optimized as follows. The ROUND parameter in FIND is set to ± 2, such that stars with any long-width ratio will be accepted. In order to reduce the number of false detections, the Hmin parameter should be increased properly. Based on experimental experiences, we set Hmin to $25 + \text{background}(H)$, which means that the H value of Peak points should be at least 25 higher than that of the background. Readers can refer to Stetson (1987) for detail of the parameters ROUND and Hmin. In one word, we use the DAOPHOT FIND routine with proper parameters to find peak points.

Figure 2 shows the results of each step of our method. The left image illustrates the result of the step of searching peak points. It results from the FIND routine with optimized parameters. In the image, the purple boxes represent detected stars whose centers are at the center positions of these boxes. The content in the small red box is enlarged and shown at the right top of the image. It can be seen from the image that at least one peak point is recognized for each trailed star with optimized parameters.

2.2. Step 2: Finding Streaks

With at least one peak point in each streak, the region growing algorithm is used to obtain the streak regions. The algorithm can find all pixels in the connected neighbors of a seed pixel (i.e., the peak pixel). For the details of region growing, see also Gonzalez & Woods (2002). The whole process of finding the streak region consists of six secondary steps as follows.

1. Set a threshold d and the size of a square local image n. d will be used to determine whether the region is a streak or not. n will define the size of the square local image of a peak point.
2. Given a peak point P, find out a local image $SubImg$ that is centered at P and has a size $n \times n$. If P is near the

boundary of the image, center *SubImg* as close to *P* as possible.

3. For the local image *SubImg*, compute the mean (m) and standard deviation (σ) of all pixel intensities after applying 3σ clipping criteria. Set intensity threshold $T = m + 2\sigma$.

4. The region growing algorithm is performed to expand the region around point *P* and then obtain the expanded region *R* associated with *P*. In the region, all pixels are connected and their intensity is greater than *T*. The IDL function REGIONGROW is called to finish it.

5. For each peak point P_i, repeat steps 2–4 to obtain its expanded region R_i. To avoid overlapping regions, we restrict a pixel to belonging to only one region. Generally, the restriction makes sure that one streak has only one expanded region even if it has several peak points.

6. Determine which expanded regions are streaks. Compute the maximum length of the region R_i in x, y directions that are denoted by L_x and L_y, respectively. If $\max(L_x, L_y) > d$, R_i is a streak region and saved as SR_i. Perform the same operation on every expanded region to get all streaks.

Through the above six steps, streak regions are determined. The parameters d, n and T play important roles in the whole procedure of finding streak regions. d is used to determine whether the region is a streak or not. n defines the size of the square local image *SubImg* of a peak point, and indirectly determines the intensity threshold T that affects the growth of the region from one peak point. Based on the properties of ISS images, the parameters are set as $d = 6$, $n = 128$ and $T = m + 2\sigma$. All these values work well for ISS images. In other applications, these parameters should be adjusted based on the properties of images used.

The middle image in Figure 2 shows the streaks detected from the left image with our method. It is a binary image, white regions are detected streaks. Comparing with the left image, it can be seen that the number of false detected streaks reduced significantly.

2.3. Step 3: Centering Streaks

After finding out all streak regions, an improved modified moment method is used to compute the centers of all streaks. Similar to the method described by Zhang et al. (2021), we developed a modified moment method to locate the centers of streaks. It includes three secondary steps as follows.

1. Obtain a complete streak region FR_i. The complete region should contain both foreground and background areas of a streak. We assume that it is a rectangular area. Since in most cases SR_i, which approximates the real foreground area, is an irregular area. To obtain the complete region, we first generate the bounding box of SR_i, and then

expand it outward by more k pixels. In our processing, the k is 4.

2. Update the intensities of all pixels in FR_i. In the approximate background area $FR_i - SR_i$, a 2σ clipping method is used to remove outliers to get all background pixels of a peak point. With the mean (m) and standard deviation (σ) of all background pixel intensities, another threshold $B = m + 2\sigma$ is obtained. All pixels with an intensity no greater than B in FR_i will be changed to zero.

3. Compute the center of a streak. The modified moment formulation is applied to the region FR_i to get the streak center.

The secondary steps 1–3 are repeated for each streak region to locate the centers. The right image in Figure 2 shows the results from centering streak of the left one. each purple box indicates one streak center. Although there are still false detected streaks, they will not affect the final result because they cannot be matched with catalog stars.

The above three main steps comprise the proposed automatic detecting and centering method for streaks in ISS images. In Section 4 a discussion about the method will be given.

3. Data Reduction

We collected 710 ISS images with trailed stars of several moons of Saturn that include Enceladus, Dione, Mimas, Rhea and Tethys. Sifting and discarding the incomplete or contaminated images, a total of 658 ISS images remain.

The Caviar software package (Cooper et al. 2018) is used to perform the astrometry of these images. In order to enable Caviar to process images with streaks, we integrated our automatic streak centering method into it. The whole reduction involves two key operations: pointing correction and measurement of target centers. In point correction, the catalog stars were matched with image stars to correct the nominated pointing of ISS camera. The center positions of all image stars were determined by our streak centering method proposed in the paper, and corrected with the geometric distortion model given in (Owen 2003). The catalog stars are extracted from Gaia Early Data Release 3 (Gaia Collaboration et al. 2016, 2021). In the measurement of the target's center, the limb-fitting method (Tajeddine et al. 2013) is used to get the center because targets are resolved in all ISS images. Finally, we reduced 658 ISS images, which includes 539 images of Enceladus from 2012 to 2017, 57 images of Dione, 22 images of Mimas, 14 images of Rhea and 26 images of Tethys. A sample of the results is given in Table 1. Each row shows one observation of a target. Column 1 is the ID of the reduced image. Column 2 is the observation time of the image, which is the middle time of the exposure of the image. Column 3 is the target name. Columns α, δ are the R.A. and decl. of target in ICRF (International Celestial Reference Frame) centered at

Table 1
A Sample of the Results

Image ID	Mid-time(UTC) (UTC)	Body	α (degrees)	δ (degrees)	α_c (degrees)	δ_c (degrees)	Twist (degrees)	Sample (pixels)	Line (pixels)
N1828232894	2015-342T01:24:23.436	ENCELADUS	82.083 769 9	−4.1726995	82.083 767 7	−4.1727152	3.423 695 6	504.65	892.14
N1516373834	2006-019T14:27:36.382	RHEA	319.242 799 0	−1.2519495	319.242 750 5	−1.2518827	173.716 458 2	566.94	574.44
N1532687765	2006-208T10:04:43.381	DIONE	279.777 534 0	−13.9993040	279.776 992 0	−13.9992617	264.291 353 2	508.13	516.82
N1532778115	2006-209T11:10:31.351	MIMAS	288.033 728 7	−11.9340958	288.033 692 6	−11.9341869	263.920 922 2	496.20	521.16
N1525531204	2006-125T14:09:25.071	TETHYS	324.930 220 3	−1.9154561	324.930 225 5	−1.9154309	199.480 203 9	561.18	579.10

Note. Column 1 is the Cassini ISS image ID. Column 2 is the date and exposure mid-time of the image (UTC). Columns α and δ are the R.A. and decl. in ICRF centered at Cassini for target, while α_c, δ_c, and Twist refer to the R.A., decl., and twist angle of the cameras pointing in the same coordinate system. The columns of Sample and Line are the observed positions in the image. The full table is available from the CDS. The origin of the sample, line coordinate system is at the top left of the image, and line increasing downwards and sample to the right. All the angle variables are given in degrees.
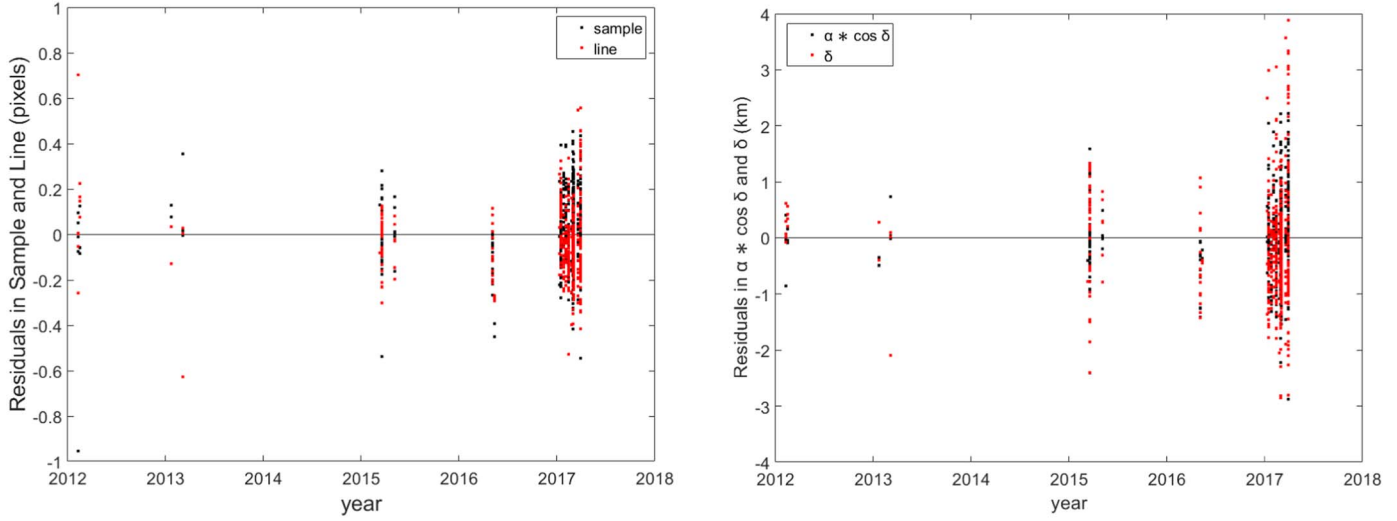
Figure 3. The residuals of Enceladus relative to JPL ephemeris SAT427 in Sample and Line (in pixels), and in $\alpha * \cos\delta$ and δ directions (in km).
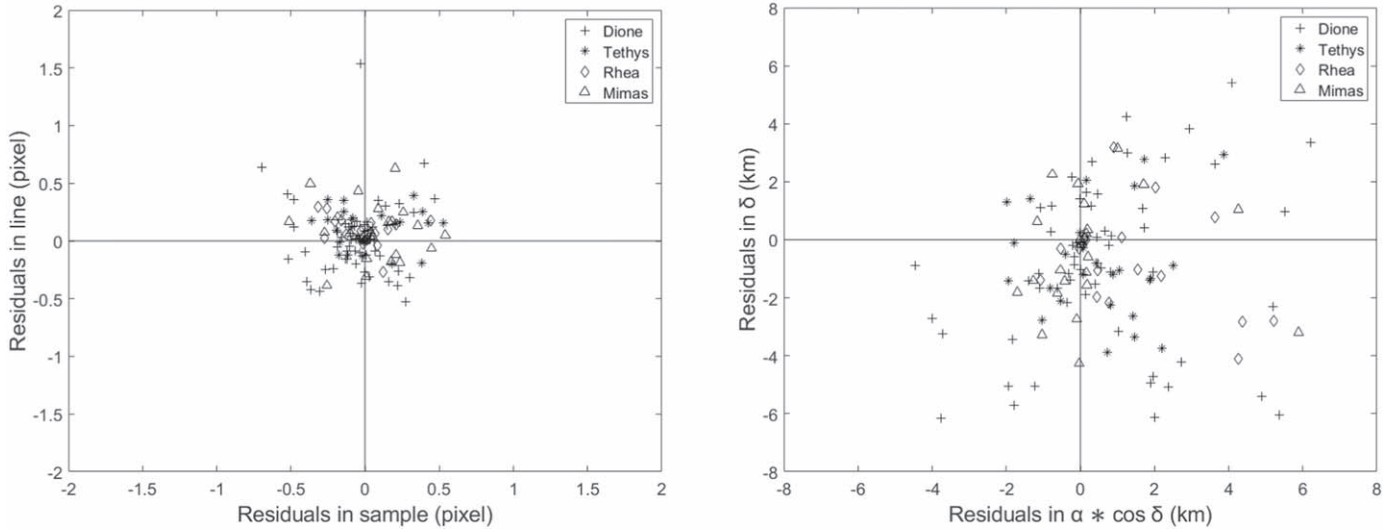
Figure 4. The residuals of Mimas, Dione, Rhea, and Tethys relative to JPL ephemeris SAT427 in Sample and Line directions (in pixels), and in $\alpha * \cos\delta$ and δ directions (in km).

Cassini. Columns α_c, δ_c and Twist are the camera's pointing in ICRF centered at Cassini. The corresponding image coordinates are given in columns Sample and Line. The full Table 1 is available at CDS via anonymous ftp to cdsarc.u-strasbg.fr (130.79.128.5) or via https://cdsarc.unistra.fr/viz-bin/cat/J/other/RAA.

4. Discussion

To evaluate our measurement, we compared our results with the JPL ephemeris SAT427 (for detail see also https://naif.jpl.nasa.gov/pub/naif/generic_kernels/spk/satellites/sat427.cmt) to get the residuals of all these observations. The residuals of Enceladus in sample and line are displayed in the left panel in Figure 3, and R.A. (α) and decl. (δ) are displayed in the right panel in Figure 3. Figure 4 shows the same residuals of other Saturnian satellites, i.e., Mimas, Dione, Rhea and Tethys.

The mean and standard deviations (SD) of these residuals are given in Table 2. It shows that the SD in sample and line of Enceladus are 0.16 pixels and 0.15 pixels, respectively. In terms of distance, the SD in R.A. and decl. are 0.69 km and 0.98 km, respectively. For the other four targets: Mimas, Dione, Tethys and Rhea, their counterparts are 0.24 pixels, 0.27 pixels, 2.02 km and 2.36 km, respectively.

Table 2
Mean Values and Standard Deviations of Residuals of Our Results Relative to the JPL Ephemeris SAT427

		Sample (pixels)	Line (pixels)	$\alpha * \cos\delta$ (arcsec)	δ (arcsec)	$\alpha * \cos\delta$ (km)	δ (km)
Enceladus	Mean	0.02	0.04	0.04	0.03	0.01	0.13
	SD	0.16	0.15	0.14	0.17	0.69	0.98
The others	Mean	0.02	0.05	0.06	0.11	0.58	0.87
	SD	0.24	0.27	0.25	0.31	2.02	2.36
Total	Mean	0.02	0.02	0.01	0.04	0.11	0.26
	SD	0.18	0.18	0.17	0.22	1.08	1.37

Note. The others include Dione, Mimas, Rhea and Tethys.

Table 2 also shows that the result of Enceladus is more precise than that of the other satellites. There are two reasons. First, the exposure times for Enceladus are generally between 5.6 and 8.2 s while for other targets are between 10 and 46 s. The longer exposure time may increase image noise and thus reduce the accuracy of position measurements. Second, the observation conditions of other satellites are more variable than those of Enceladus, which decrease the precision of the measurement.

The results show that our automatic streak centering method works well. As stated in Section 2, there are a few parameters affecting the method. On one hand, these parameters enhance the flexibility and application range of our method. On the other hand, these parameters should be set carefully because the improper parameter setting may cause the failure of the method. Our parameter setting fits the properties of our ISS images in which the reference stars are sparse, generally less than 20 in each image, and displayed as straight lines. It is because all these observations have a small field of view of $\sim 2'$, a limited magnitude of ~ 15, and steadily track the observation target. These three factors result in the reference stars being sparse and appearing as straight lines.

It should be pointed out that not all streak regions detected by our method are true. That is, there are some false streak detections in an ISS image. However, it does not influence the result because all true streaks will be matched with catalog stars while the false detections will be filtered out.

The disadvantage of the method is that it cannot provide the accurate center position for a curved streak. In physical view, the modified moment method only works out the first-order moment center of an intensity distribution. For a non-straight streak, the geometric center is not what we desired. It requires further research on centering curved streaks. Fortunately, all trailed stars appear as straight streaks in all images of our targets.

5. Conclusion

In this paper, a method is proposed to automatically search streaks and determine their accurate centers. The method is applied to measure 658 ISS images of several main moons of Saturn with streaks, 539 of these images are Enceladus, and the remaining images are Mimas, Dione, Tethys and Rhea. The final results show that the proposed method is efficient. Compared with the JPL ephemeris SAT427, mean residuals of all measurements of Enceladus are 0.02 pixels in sample and 0.04 pixels in line, with standard deviations of 0.16 and 0.15 pixels, respectively. In terms of distance, the mean residuals of Enceladus are 0.01 km in $\alpha \times \cos(\delta)$ and 0.13 km in δ, with standard deviation smaller than 1 km. For the other four targets, the means and standard deviations of their residuals are worse than Enceladus because of the different observation conditions. Overall, in terms of residuals in linear units, the means in the R.A. and decl. are 0.11 and 0.26 km, respectively; The standard deviations are 1.08 and 1.37 km, respectively.

ORCID iDs

Yan Li ⬤ https://orcid.org/0000-0001-7372-100X

References

Cooper, N. J., Lainey, V., Meunier, L. E., et al. 2018, A&A, 610, A2
Cooper, N. J., Murray, C. D., Lainey, V., et al. 2014, A&A, 572, A43
Cooper, N. J., Murray, C. D., Porco, C. C., & Spitale, J. N. 2006, Icarus, 181, 223
Cooper, N. J., Renner, S., Murray, C. D., & Evans, M. W. 2015, AJ, 149, 27

Denneau, L., Jedicke, R., Grav, T., et al. 2013, PASP, 125, 357
Desmars, J., Li, S. N., Tajeddine, R., Peng, Q. Y., & Tang, Z. H. 2013, A&A, 553, A36
Fraser, W., Alexandersen, M., Schwamb, M. E., et al. 2016, AJ, 151, 158
Gaia Collaboration, Brown, A. G. A., Vallenari, A., et al. 2021, A&A, 649, A1
Gaia Collaboration, Prusti, T., de Bruijne, J. H. J., et al. 2016, A&A, 595, A1
Gonzalez, R. C., & Woods, R. E. 2008, Digital Image Processing (3rd ed; Hoboken, NJ: Pearson), 763
Laas-Bourez, M., Blanchet, G., Boër, M., Ducrotté, E., & Klotz, A. 2009, AdSpR, 44, 1270
Lainey, V., Casajus, L. G., Fuller, J., et al. 2020, NatAs, 4, 1053
Lainey, V., Jacobson, R. A., Tajeddine, R., et al. 2017, Icarus, 281, 286
Owen, W., Jr 2003, JPLIOM, 312

Porco, C. C., West, R. A., Squyres, S., et al. 2004, SSRv, 115, 363
Sease, B., Flewelling, B., & Black, J. 2017, AcAau, 134, 345
Stetson, P. B. 1987, PASP, 99, 191
Sun, R.-Y., Zhao, C.-Y., & Zhang, Y.-P. 2013, PASJ, 65, 110
Tajeddine, R., Cooper, N. J., Lainey, V., Charnoz, S., & Murray, C. D. 2013, A&A, 551, A129
Tajeddine, R., Lainey, V., Cooper, N. J., & Murray, C. D. 2015, A&A, 575, A73
Virtanen, J., Poikonen, J., Säntti, T., et al. 2016, AdSpR, 57, 1607
Zhang, Q. F., Lainey, V., Cooper, N. J., et al. 2018, MNRAS, 481, 98
Zhang, Q. F., Qin, W. H., Ma, Y. L., et al. 2022, Planet. Space Sci., 221, 105553
Zhang, Q. F., Zhou, X. M., Tan, Y., et al. 2021, MNRAS, 505, 5253